New Emulsion Polymerization Tubular Reactor with Internal Angular Baffles: Reaction Temperature Effect

Florentino L. Mendoza Marín,[1] Liliane Maria Ferrareso Lona,[2] Maria R. Wolf Maciel,[1] Rubens Maciel Filho[1]

[1]*Laboratory of Optimization, Design and Advanced Process Control (LOPCA), Faculty of Chemical Engineering, State University of Campinas (UNICAMP), Campinas, SP, Brazil*
[2]*Laboratory of Analysis and Simulation of Chemical Process, Department of Chemical Processes, Faculty of Chemical Engineering, State University of Campinas (UNICAMP), Campinas, SP, Brazil*

Received 20 April 2005; accepted 15 July 2005
DOI 10.1002/app.22638
Published online 2 February 2006 in Wiley InterScience (www.interscience.wiley.com).

ABSTRACT: Deterministic models of physicochemical, mathematical, and computational sciences were used for modeling and simulation of emulsion homopolymerization process of styrene with baffles into tubular reactor (TR) as static mixer. Modeling and simulation were approximate to steady state, cylindrical one-dimensional model, fully developed laminar plug flow, and they were solved with finite volume method and programmed with Fortran language. Also, the Smith-Ewart model was considered to estimate the monomer conversion and Arrhenius chemical kinetics was considered as laminar finite-rate model to compute chemical source. The experimental-inductive and mathematical-deductive methods were applied for obtaining mass balance results and properties characterization. The objective is to model, to simulate, and to analyze the emulsion polymerization reactor performance with internal-inclined angular baffles, and to compare with continuous TR in variable reaction temperature. The predictions were validated with experimental results for the isothermic and TR, with a good concordance. The results in no isothermal conditions without and with baffles were better than in isothermal conditions without and with baffles in relation to the desired properties. © 2006 Wiley Periodicals, Inc. J Appl Polym Sci 100: 2572–2581, 2006

Key words: modeling; simulating; emulsion polymerization; tubular reactor; baffles

INTRODUCTION

Plastics, as synthetic polymers, are major chemical industry goods used in the building, construction, packing, transportation, electronic, appliances, etc. Polymers are products of big importance in the current society, with a market in significant expansion and the demands of products with required specifications by its applications. Polystyrene belongs to the group of standard thermoplastics. Its annual consumption increases every year. It is one of the most important polymers, and its industrial production is carried out exclusively by a free-radical mechanism. The fundamentals of emulsion polymerization are sufficiently well understood such that new products can be made and old ones reformulated. An example is the economical and technical importance to produce a submicron suspension of colloidally stable polymer particles or latex with 40–50%, by free-radical mechanism of the total polymer. It is a heterogeneous reaction process in which unsaturated monomers or monomer solutions are dispersed in a continuous phase with the aid of an emulsifier system and polymerized with free-radical initiators.[1–4] Emulsion polymerization process is a complex heterogeneous process involving transport of monomer, free radicals, and other species between aqueous and organic phases, compared to other heterogeneous polymerizations (suspension or precipitation); it is likely the most complicated system. All these factors make modeling of this system very difficult.[5,6]

The chemical processes have growing operational difficulties caused by the diversification and specification of products, and investigations for alternative reactors projects and analysis of their behavior under static and dynamic conditions are welcome. In conventional tubular reactor (TR), most reaction happens towards the reactor entrance, and the variable reaction for exothermic reactions as well as the limitations to heat transfer near the wall makes the behavior to be very complex.[7–10]

Bearing this in mind, in this work, an alternative TR based on the placement of the baffles inside the reactor for emulsion polymerization of styrene (EPS) is proposed. The objective is to model, simulate, and analyze the emulsion polymerization reactor performance

Correspondence to: F. L. M. Marín (maciel@feq.unicamp.br).
Contract grant sponsor: PEC-PG/CAPES.
Contract grant sponsor: LOPCA-DPQ/FEQ UNICAMP.

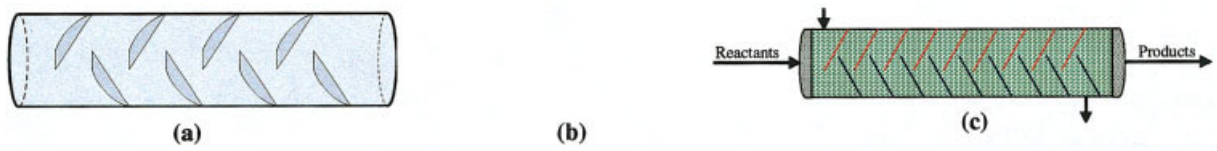

Figure 1 (a) Schematic representation of polymerization TR with baffles. (b) Area of baffle; Bb is base of the baffle, Lb is length of the baffle. (c) Profile of polymerization TR with internal inclined angular baffles. [Color figure can be viewed in the online issue, which is available at www.interscience.wiley.com.]

with internal inclined angular baffles on variable reaction temperature effect. The products were characterized with particles number (homogeneous nucleation (HN) and heterogeneous nucleation), molecular weight distribution, polymer particles size, and polymer viscosity distribution. These results were validated with literature results under same or approximate conditions. The results for the no isothermal conditions were better than in isothermal conditions without or with baffles in relation to the desired properties.

REACTIONAL SYSTEM

Conditions of test

To evaluate the performance of the proposed design, the EPS is considered, and comparison with conventional TR is carried out. Figure 1 shows the alternative proposed reactor. To represent the system, a simplified one-dimensional deterministic model is developed with the following assumptions: flow along the axial direction (negligible diffusion); fully developed axial velocity of fluid flow; polymer particle phase is the main locus of polymerization; particle size is monodisperse; the monomer conversion is estimated by Smith–Ewart model, and Arrhenius chemical kinetics as laminar finite-rate model to compute chemical source.

Properties

To evaluate the performance of the proposed alternative reactor design, the EPS was considered; specifically, the work of Bataile et al.[11] that conducted emulsion homopolymerization of styrene at 60°C with potassium persulfate (KPS), 0.026 mol/L; sodium dodecyl sulfate (SDS), 0.070 mol/L; styrene, 8.39 mol/L; and water 161.52 mol/L. More information of the bibliographical references of the properties and parameters (given in Table I) can be found in Mendoza Marín.[12]

MATHEMATICAL MODELING

To represent the proposed reactor shown in Figure 1, with the case study of emulsion homopolymerization of styrene, the following model equation may be written.

Chemical reaction

The mechanism of EPS may be schematized and briefly shown as:

$$\text{Initiation: } I_2 \xrightarrow{Kd} 2I^- \quad I^- + M \xrightarrow{Kp} R_1 \tag{1}$$

Radical absorption by micelles (micellar nucleation (MN))

Diffusion in the water phase

$$R_{rw} \xrightarrow{Kcmw} R_{rw}MIC$$

Absorption in the micelle surface

$$R_r + MIC \xleftrightarrow{Kcm:Kcmd} R_rMIC \tag{2}$$

Radical absorption by particles (HN)

Diffusion in the water phase

$$R_{rw} \xrightarrow{Kcpw} R_{rw}PP$$

Absorption in the particle surface

$$R_r + PP \xleftrightarrow{Kcp:Kcpd} R_rPP \tag{3}$$

$$\text{Propagation: } R_r + M \xrightarrow{Kp} R_{r+1} \tag{4}$$

Termination: by combination (Ktc) and disproportionation (Ktd)

TABLE I
Physical, Chemical, Mechanical, Transport, Rheological, Thermodynamic, and Geometrical (Grid, Particles, Reactor, Baffles) Properties of Styrene as Database for Simulation of EPS

Symbol	Value, unit, and description
Na	6.02×10^{23} molecules/mol; Avogadro's number; $\pi = 3.14159$
Rg	1.987 cal/mol K; gas constant
ρ_p and ρ_m	l.25–0.0004202T kg/L, polymer density; 0.949–0.00128 ($T-273.15$) kg/L, monomer density
anrp	0.5; average number of radicals per particle
CMC	0.008 (mol/L); critical micelle concentration
CMw	0.005 (mol/L); monomer concentration in water phase (=Mw)
Fi	0.5; initiator efficiency
Kcm	$4\pi \mathrm{Dwr}_{\mathrm{mic}} N_A$ (1/min); rate constant of aqueous phase radical capture by micelles
Kcp	$4\pi \mathrm{Dpr}_p N_A$ (1/min); rate constant of radicals capture by polymer particles
Kd	$1.524 \times 10^{18} \exp(-33320/\mathrm{Rg}T)$ (1/min); rate constant of initiator decomposition
Kp	$4.703 \times 10^{11} \exp(-9805/\mathrm{Rg}T)$ (L/mol min); rate constant of propagation of polymer particles
Kt	$1.04619 \times 10^{10} \exp(-2950{,}45/\mathrm{Rg}T)$ (L/mol min); global rate constant for termination
$[\mathrm{M}]_p$	$(1-\phi_p)\rho_m/\mathrm{MWs}$ (mol/L); monomer concentration in polymer particle
MWe	288.38 g/mol; molecular weight of surfactant
MWi	271.3 g/mol; molecular weight of initiator
MWs	104 g/mol; molecular weight of styrene
Ncr	5; critical chain length at which water phase radical can be absorbed
Nem	60 (No.Emul/mic); number of emulsifier molecules in a micelle
Sa	3×10^{-17} dm^2; area covered by one molecule of emulsifier
ϕ_p and ϕ_m	0.4, volume fraction of polymer; 0.6, volume fraction of monomer
Re	5000 (laminar) and 13,600 (turbulent) Reynolds number
v_{in}	0.27027 (laminar) and 0.7351 (turbulent) (m/min) inlet velocity in TR
D_p	1.76×10^{-12} dm^2/min; diffusivity of monomer radicals in polymer phase
D_w	1.76×10^{-9} dm^2/min; diffusivity of monomer radicals in water phase
μ	0.001 kg/m s; viscosity of polymer
T_{in}	333.15 and 363.15 (K); inlet temperatures to the reactor
ΔH	−16682.2 cal/mol; polymerization reaction heat of styrene
N	51; number of nodal points
r_{mic}, r_p	27.5 Å, radius of micelle; 275 Å, radius of polymer
Dr, Lr	1 m, diameter of TR; 20 m, length of TR
Lbr	1 m, length of baffle separation; Nb = 6, 18 number of baffles

$$R_n + R_m \xrightarrow{\mathrm{Ktc}} P_{n+m} \text{ or } R_n + R_m \xrightarrow{\mathrm{Ktd}} P_n + P_m \qquad (5)$$

Conservative models

Principle of mass conservation, in general, form for a chemical species j reacting in a flowing fluid with varying density, temperature, and composition is

$$\frac{\partial C_i}{\partial t} + \nabla \cdot (C_j \bar{u}) + \nabla J_j = R_j \qquad (6)$$

where C_j is the molar concentration of species j; $\partial C_j/\partial t$ is the nonsteady-state term expressing accumulation or depletion; ∇ is the gradient operator; $\nabla \bar{u}$ is the divergence of a vector function $\bar{u}$; $\bar{u}$ is the three-dimensional mass–average velocity vector; $\nabla \cdot (C_j \bar{u})$ is the transport of mass by convective flow; J_j is the molar flux vector for species j with respect to the mass–average velocity; ∇J_j is molecular diffusion only; R_j is the total rate of change of the amount of j because of reaction. Species j occurs in liquid phase. The equation can be taken in single-phase or "homogeneous" or "pseudohomogeneous" reactors.[12,13]

The generalized laminar finite-rate model was applied to compute the chemical source terms (R_j). The model is exact for laminar flow, but is generally inaccurate for turbulent requirements because of highly nonlinear Arrhenius chemical kinetics. The net source of chemical species j due to reaction R_j is computed as the sum of the Arrhenius reaction sources over the Ni reactions that the species participate in:

$$R_j = \sum_{i=1}^{Ni} R_{j,i} = \sum_{i=1}^{Ni} \left(K_{f,i} \prod_{i=1}^{Ni} [C_{j,i}]^{n_{fj,i}} - K_{b,i} \prod_{i=1}^{Ni} [C_{j,i}]^{n_{bf,i}} \right) \qquad (7)$$

where $R_{j,i}$ is the Arrhenius molar rate of creation/destruction of species j in reaction i; $K_{f,i}$ is the forward rate constant for reaction i, $K_{b,i}$ is the backward rate constant for reaction i, Ni is the number of chemical species in reaction i, $C_{j,i}$ is the molar concentration of each reactant and product species j in reaction i, $n_{fj,i}$ is the forward rate exponent for each reactant and product species j in reaction i, $n_{bj,i}$ is the backward rate

exponent for each reactant and product species j in reaction i. Only nonreversible reactions were considered and the mass balance of equations gives the different chemical source terms as free radical (R_{Rw}), initiator (R_I), monomer (R_M), surfactant ($R_E = 0$, by to be inert), and polymer (R_P):

$$R_{\mathrm{Rw}} = R_I - R_I\left[\frac{\mathrm{Kp}M_w}{\mathrm{Kp}M_w + \mathrm{Kcp}[N_P] + \mathrm{Ktw}[R]_w}\right]^{ncr-1} - \mathrm{Kcp}[N_p][R]_w Kcm[MIC][R]_w - \mathrm{Ktw}[R]_w^2 \quad (8)$$

$$R_I = -fi\mathrm{Kd}[I]_w \quad (9)$$

$$R_M = -\frac{\mathrm{Kp}[M]_p N_P \bar{n}}{N_A V_P} - \mathrm{Kpw}[M]_w[R]_w \quad (10)$$

$$R_P = \frac{\mathrm{Kp}[M]_p N_P \bar{n}}{N_A V_P} + Kpw[M]_w[R]_w \quad (11)$$

Newton's second law of momentum was applied to a small volume element moving with the fluid that is accelerated because of the forces acting over it. The motion equation in terms of τ is

$$\rho\frac{D\bar{u}}{Dt} = -\nabla P + (\nabla:\bar{\tau}) + \rho\cdot\bar{g} \quad (12)$$

where $\bar{g}$ represent the body forces per unit area; ρ is the density; P is the pressure; $\bar{\tau}$ is the extra stress tensor, and D/Dt is the material or substantial derivative.[12–14]

Principle of energy conservation in the following form shows the phenomenon that is of importance in reactors

$$\sum_j \overline{M}_j C_j c_{Pj}\left(\frac{\partial T}{\partial t} + \bar{u}\nabla T\right) = \sum_i (-\Delta H_i) r_i + \nabla\cdot(\lambda\nabla T) - \sum_j J_j \nabla H_j + Q_{rad} \quad (13)$$

where c_{pj} is the specific heat of species j; λ is the thermal conductivity of the mixture; $\underline{H}_j$ are partial molar enthalpies; T is the temperature; $\overline{M}_j$ is molecular mass of species j; and Q_{rad} is heat of radiation.[15] By taking into account the flow in the axial direction and the steady state and by neglecting the heat transfer by radiation as well as the molecular diffusion, the following equation can be written:

$$\rho c_p v_z \frac{\partial T}{\partial z} = (-\Delta H) r \quad (14)$$

$$r = R_M = -\mathrm{Kpo}\exp\left(-\frac{\mathrm{Ep}}{\mathrm{Rg}T}\right)\frac{[M]_p N_P \bar{n}}{N_A V_P} \quad (15)$$

where $\rho = \sum_i \bar{M}_j C_j$; $\sum_i(-\Delta H_i)_r = (-\Delta H)_r$; ρ is polymer density; Ep is activation energy of styrene propagation; Np is total number of polymer particles; and $\tilde{n}$ is average number of radicals per particle. Equations (14) and (15) were solved with finite volume method (FVM) to calculate axial temperature distribution and other variables, such as concentration (initiator, free radicals, monomer, polystyrene), velocity, particle number, etc., simultaneously with iterative procedure.

In the MN is accepted that particles are generated by micelle absorbing radicals from the water phase where R_{MN} is the rate of particle formation by MN (see mechanism).

$$R_{\mathrm{MN}} = \frac{d[\mathrm{Np}]_m}{dt} = \mathrm{Kcm}[\mathrm{MIC}][R]_w \quad (16)$$

Formation rate for the first oligomeric radicals in the aqueous phase (see mechanism) is

$$\frac{d[R_1]_w}{dt} = R_l - \mathrm{Kp}\cdot\mathrm{Mw}\cdot[R_1]_w - \mathrm{Kcm}\cdot[\mathrm{MIC}][R_1]_w - \mathrm{Ktw}\cdot[R]_w[R_1]_w \quad (17)$$

Formation rate for the ith oligomeric radicals in the aqueous phase (see mechanism) is

$$\frac{d[R_i]_w}{dt} = \mathrm{Kp}\cdot\mathrm{Mw}\cdot[R_{i-1}]_w - \mathrm{Kp}\cdot\mathrm{Mw}[R_i]_w - \mathrm{Kcm}\cdot[MIC] \times [R_i]_w - \sum_{j=1}^{\infty}\mathrm{Kcp}_j[\mathrm{Np}_j][R_i]_w - \mathrm{Ktw}\sum_{j=1}^{\mathrm{ncr}-1}[R_i]_w[R_j]_w \quad (18)$$

$$\text{Definition: } \sum_{j=1}^{\infty}\mathrm{Kcp}_j[\mathrm{Np}_j] = \mathrm{Kcp}[\mathrm{Np}] \quad (19)$$

Formation rate of total oligomeric radicals in the aqueous phase ($[\mathrm{R}]_w$)

$$\sum_{j=1}^{\mathrm{ncr}-1}[R_j]_w = [R]_w \quad (20)$$

If the steady state hypothesis is applied to all radicals in the water phase, i.e., setting left-hand side of eqs. (17) and (18) to zero, one obtain the following equations:

$$[R_1]_w = \frac{R_l}{\mathrm{KpMw} + \mathrm{Kcm}[\mathrm{MIC}] + \mathrm{Ktw}[R]_w} \quad (21)$$

$$[R_i]_w = \frac{\mathrm{KpMw}[R_{i-1}]_w}{\mathrm{KpMw}+\mathrm{Kcm}[\mathrm{MIC}]+\mathrm{Ktw}[R]_w + \mathrm{Kcp}[\mathrm{Np}]} \tag{22}$$

The probability for the formation of oligomeric radical by micelle propagation (α_m) is written as:

$$\alpha_m = \frac{\mathrm{KpMw}}{\mathrm{KpMw}+\mathrm{Kcm}[\mathrm{MIC}]+\mathrm{Ktw}[R]_w + \mathrm{Kcp}[\mathrm{Np}]} \tag{23}$$

Equation (22) can then be rewritten and solve for all oligomer

$$[R_i]_w = \alpha_m[R_{i-1}]_w = \alpha_m\alpha_m[R_{i-2}]_w$$

$$= \alpha_m\alpha_m\alpha_m[R_{i-3}]_w = \cdots = \prod_{i=1}^{\mathrm{ncr}-1} \alpha_m^i[R_1]_w \tag{24}$$

$$[R_i]_w = \alpha_m^{\mathrm{ncr}-1}[R_1]_w \tag{25}$$

Substituting eq. (21) into eq. (25) gives

$$[R_i]_w = \frac{R_l}{\mathrm{KpMw}+\mathrm{Kcm}[\mathrm{MIC}]+\mathrm{Ktw}[R]_w}\,\alpha_m^{\mathrm{ncr}-1} \tag{26}$$

The following definitions are used to simplify symbols. Total radical concentration in the aqueous phase

$$[R]_w = \sum_{i=1}^{\mathrm{ncr}-1} [R_i]_w \tag{27}$$

Substituting eq. (26) into eq. (27) gives

$$[R]_w = \frac{R_l}{\mathrm{KpMw}+\mathrm{Kcm}[\mathrm{MIC}]+\mathrm{Ktw}[R]_w} \sum_{i=1}^{\mathrm{ncr}-1} \alpha_m^{\mathrm{ncr}-1} \tag{28}$$

The geometric progression is applied to the end term of eq. (28)

$$\sum_{i=1}^{n-1} x^{i-1} = \frac{1-x^{n-1}}{1-x} \tag{29}$$

Equation (28) can be then rewritten and gives the total radical concentration in the aqueous phase.

$$[R]_w = \frac{R_l}{\mathrm{KpMw}+\mathrm{Kcm}[\mathrm{MIC}]+\mathrm{Ktw}[R]_w}\left(\frac{1-\alpha_m^{\mathrm{ncr}-1}}{1-\alpha_m}\right) \tag{30}$$

The final equation of the rate of particle formation for MN is then

$$R_{\mathrm{MN}} = \frac{d[\mathrm{Np}]_m}{dt}$$

$$= \frac{\mathrm{Kcm}[\mathrm{MIC}]R_l}{\mathrm{KpMw}+\mathrm{Kcm}[\mathrm{MIC}]+\mathrm{Ktw}[R]_w}\left(\frac{1-\alpha_m^{\mathrm{ncr}-1}}{1-\alpha_m}\right) \tag{31}$$

In the HN is accepted that the particles could be generated by precipitated water-phase oligomer radicals, where R_{HN} is the rate of particle formation by HN (see mechanism), and it can be written as:

$$R_{\mathrm{HN}} = \frac{d[\mathrm{Np}]_h}{dt} = \mathrm{KpM}_w[R_{\mathrm{ncr}-1}]_w \tag{32}$$

Formation rate for first oligomeric radicals in the aqueous phase (see mechanism)

$$\frac{d[R_1]_w}{dt} = R_l - \mathrm{KpMw}[R_l]_w - \sum_{j=1}^{\infty}\mathrm{Kcp}_j[\mathrm{Np}_j][R_1]_w$$

$$- \mathrm{Ktw}\sum_{j=1}^{\mathrm{ncr}-1}[R_j]_w[R_1]_w \tag{33}$$

Formation rate for ith oligomeric radicals in the aqueous phase (see mechanism)

$$\frac{d[R_t]_w}{dt} = \mathrm{kpMw}[R_{i-1}]_w - \mathrm{kpMw}[R_i]_w$$

$$- \mathrm{Kcp}[\mathrm{Np}][R_i]_w - \mathrm{Ktw}[R]_w[R_i]_w \tag{34}$$

If the steady state is applied to all radical in the water phase, the following equations are obtained:

$$[R_1]_w = \frac{R_l}{\mathrm{KpMw}+\mathrm{Kcp}[\mathrm{Np}]+\mathrm{Ktw}[R]_w} \tag{35}$$

$$[R_i]_w = \frac{\mathrm{KpMw}[R_{i-1}]_w}{\mathrm{kpMw} + Ktw[R]_w + Kcp[Np]} \tag{36}$$

The probability for the formation of oligomeric radicals by homogeneous propagation (α_h) is written as:

$$\alpha_h = \frac{\mathrm{kpMw}}{\mathrm{kpMw} + Ktw[R]_w + Kcp[Np]} \tag{37}$$

Equations (35) and (36) can then be rewritten and solve for all radical oligomer

$$[R_1]_w = \frac{R_l}{\mathrm{kpMw}}\alpha_h \tag{38}$$

$$[R_i]_w = \alpha_h[R_{i-1}]_w = \alpha_h\alpha_h[R_{i-2}]_w = \alpha_h\alpha_h\alpha_h[R_{i-3}]_w = \cdots = \prod_{i-1}^{\text{ncr}-1} \alpha_h^l[R_1]_w \quad (39)$$

Substituting eq. (38) into eq. (39) gives

$$[R_i]_w = \alpha_h^{\text{ncr}-1}[R_l]_w = \frac{R_1}{\text{kpMw}}\alpha_h^{\text{ncr}} \quad (40)$$

Definition of radicals where chain length at the critical chain length (ncr). The last propagation step involving a radical of chain length ncr-1 and a monomer can actually be considered as the particle formation step.[3,6] Applying this definition to eq. (40) gives

$$[R_{\text{ncr}-1}]_w = \frac{R_l}{\text{kpMw}}\alpha_h^{\text{ncr}-1} \quad (41)$$

Substituting eq. (41) into eq. (32) gives the final equation of the rate of particle formation by HN

$$R_{\text{HN}} = \frac{d[\text{Np}]_h}{dt} = R_l\alpha_h^{\text{ncr}-1} \quad (42)$$

Characterization of polymer particle

The polymer particle number (by MN and HN) is determined with eq. (6) written like eq. (43) and source term as eq. (44):

$$\frac{\partial C_{N_p}}{\partial t} + \left(v_r\frac{\partial C_{N_p}}{\partial r} + v_0\frac{1}{r}\frac{\partial C_{N_p}}{\partial \theta} + v_z\frac{\partial C_{N_p}}{\partial z}\right) = D_{NB}\left(\frac{1}{r}\frac{\partial}{\partial r}\left(\frac{\partial C_{N_p}}{\partial r}\right) + \frac{1}{r^2}\frac{\partial^2 C_{N_p}}{\partial \theta^2} + \frac{\partial^2 C_{N_p}}{\partial z^2}\right) + R_{N_p} \quad (43)$$

$$R_{\text{N}_\text{p}} = R_{\text{MN}} + R_{\text{HN}} = \frac{\text{Kcm[MIC]}R_l}{\text{kpMw+Kcm[MIC]+Ktw}[R]_w}\left(\frac{1-\alpha_m^{\text{ncr}-1}}{1-\alpha_m}\right) + R_l\alpha_h^{\text{ncr}-1} \quad (44)$$

The molecular weight distribution is determined with mechanism of EPS. Moments of molecular weigh distribution and the techniques of solution of kinetic and statistical solution can solve the polymerization reaction. The kinetic solution includes direct sequential solution, discrete transformation method, and moments method. The discrete transformation method includes the steps of chemical reaction, kinetic equation, integration, expansion in power series, drop operator, and applied moments. The kinetic equation is solved through the generating function. The cumulative dead polymer were number-average molecular weight (M_n^c) and weight–average molecular weight (M_w^c):

$$M_n^c = \frac{2a\text{MWs}}{a-b}\frac{X_j}{Ln\left(\frac{b-aX_j}{b}\right)}$$

$$M_w^c = \text{MWs}\left(\frac{a+2b}{b-a} - \frac{3a}{2(b-a)}X_j\right) \quad (45)$$

where

$$a = \text{Kp}[M] \qquad b = a + \text{Ktc}[R]_w \quad (46)$$

The average swollen (Rs) and unswollen (R) particle polymer size radii[1] are

$$R_s = \left(\frac{3}{4\pi\rho_p\phi_P}\frac{\text{MW}_p C_{Ps}}{N_A C_{N_p}}\right)^{1/3}$$

$$R = R_s\left(\frac{\rho_m}{\rho_m + [M]_p\text{MW}_m}\right)^{-1/3} \quad (47)$$

The viscosity of polymer (μ) was estimated[16] as:

$$ln(\mu) = -13{,}04 + \frac{2013}{T} + \text{MW}_p^{0{,}18} \times \left[3{,}915X_j - 5{,}437X_j^2 + \left(0{,}623 + \frac{1387}{T}\right)X_j^3\right] \quad (48)$$

Reactor and baffle: geometry effect

The internal transversal areas over or beneath baffles were calculated through geometric equation. In such equation, α is the increment angle from the TR center point until total diameter, θ is the increment angle to calculate the fluid flow area of EPS beneath or over the baffles, Avb is fluid flow variable area inside TR beneath or over baffles, Ar is the area of TR without baffles and Afb is the fixed area inside TR over or beneath baffles. Figure 2 shows the variation of the transversal area available to the reactant flow inside the reactor.

$$ar(1) = \text{arcsen}\left(2\frac{ID(1)}{\text{Dr}}\right)[rad] \quad (49)$$

$$\theta r(1) = \frac{\pi}{180}\theta g(1) = \pi\left(1 - 2\frac{ar(1)}{\pi}\right)[rad] \quad (50)$$

$$\text{Avb}(1) = \frac{\text{Dr}^2}{8}(\theta r(1) - \text{sen}{-}r(1)) \quad (51)$$

$$\text{Afb}(1) = \text{Ar} - \text{Avb}(1) = \frac{\pi}{4}D_r^2 - \text{Avb}(1) \quad (52)$$

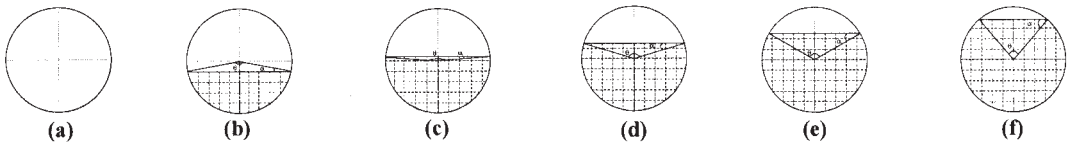

Figure 2 Variation of transversal area of fluid flow of EPS inside TR beneath or over baffles.

Calculus of Avb from $I = 2$ to number of areas beneath or over baffles (Nab)

$$\mathrm{Dvb}(1) = \mathrm{Dvb}(I-1) + \Delta\mathrm{Dvb} \tag{53}$$

$$ar(1) = \mathrm{arcsen}\left(2\frac{ID(l)}{\mathrm{Dr}}\right) = \mathrm{arcsen}\left(\frac{2}{\mathrm{Dr}}(\mathrm{Dvb}(l) - 0.5 \times \mathrm{Cr})\right) \tag{54}$$

$$\theta r(l) = \frac{\pi}{180}\theta g(1) = \pi\left(1 - \frac{2}{\pi}\alpha r(1)\right) \tag{55}$$

$$\mathrm{Afb}(l) = \frac{Dr^2}{8}(\theta r(1) - \mathrm{sen}\theta r(1)) \tag{56}$$

$$\mathrm{Avb}(l) = \mathrm{Ar} - \mathrm{Afb}(l) \tag{57}$$

The axial velocity like at TR inlet over or beneath baffles and temperature effects were estimated from Newton's second law of momentum and continuity equation. In the equation, v_{in} is the axial velocity at TR inlet in isothermal condition, v_b is the axial velocity over or beneath baffles in isothermal condition and v_z is the axial velocity in no isothermal condition [Fig. 2(a–f)].

$$v_{in} = \frac{\mu.R_e}{\rho.D_r} \qquad v_b = \frac{\mu.A_rR_e}{\rho.A_{vb}D_r} \qquad v_z = \frac{\mu.V_{z0}\rho_0}{\rho} \tag{58}$$

The FVM was used as numerical method[13,14,17] to solve the conservative balance equations. Thomas algorithm as direct method and iterative procedures were used to solve the system of resulting algebraic equations of the discretizations.

RESULTS AND DISCUSSION

The simulation results of conversion (Xj) versus length of the reactor (Z) for styrene without baffles (C0, V0) and with baffles (C6, V6) in isothermal (C) and no isothermal (V) condition are displayed in Figure 3. The conversion in no isothermal condition is better than that in isothermal condition, and the conversion increases when the baffle numbers increase. The comparative results in isothermal condition at 60°C of computational conversion (XcC), experimental conversion (Xe), and simulation conversion (literature results) (Xs) versus residence time (t) inside TR are shown in Figure 3(c). The experimental conversion has equal isothermal temperature and properties as computational conversion, but the simulation conversion has different mathematical model. The experimental and simulation conversions were those presented by Bataile et al.[11] It can be observed that the three curves have the same behavior. These comparisons allow concluding that the FVM is suitable solution method for the system.

The results for the internal transversal area (A_z) and axial velocity (v_z) along the reactor length (z) for styrene without baffles (Nb = 0) and with baffles (Nb = 6) in isothermal and no isothermal conditions are shown in the Figure 4. The positioning of transversal area inside TR can be observed as shown in Figure 4(a). The axial velocities are shown like the temperature distribution effect without baffles [Fig. 4(b)] and its localizations inside TR with baffles [Fig. 4(c)].

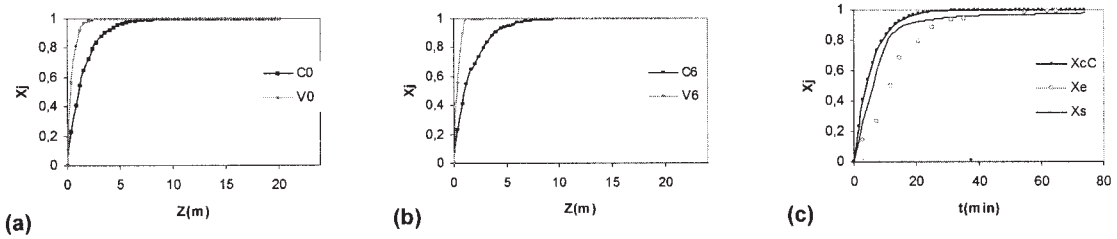

Figure 3 Conversion of monomer (a) without baffles (Nb = 0) and (b) with baffles (Nb = 6), both in isothermal (C) and no isothermal (V) conditions. (c) Experimental validation in isothermal conditions (60°C).

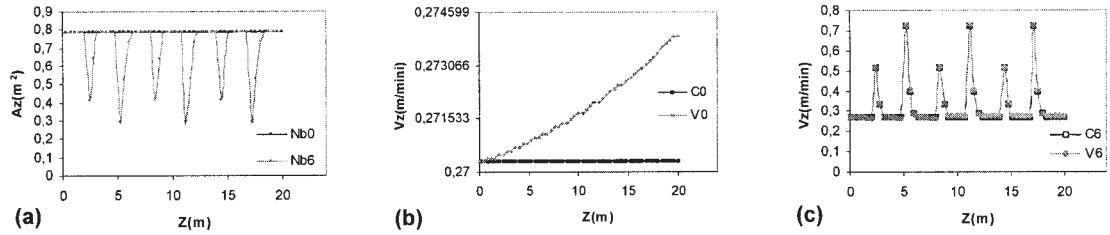

Figure 4 (a) Internal transversal area without baffles (Nb = 0) and with baffles (Nb = 6). (b) Axial velocity by the temperature effect without baffles. (c) Axial velocity distribution with baffles in isothermal (C) and no isothermal (V) conditions.

The simulation results of the polystyrene particles number (Np) by MN and HN mechanism versus length of the reactor (*Z*) without (C0, V0) and with baffles (C6, V6) in isothermal (C) and no isothermal (V) conditions were shown in Figure 5. The particle number in no isothermal condition was better than the particle number in isothermal condition without and with baffles as shown in Figure 5(a–b). The experimental (Npe) and simulation (Nps) of the particle numbers without baffles inside batch reactor versus time (*t*) is depicted in Figure 5(c). Its experimental and simulation conditions are feed temperature of 50°C, KPS 0.011 mol/L, SDS 0.05 mol/L, and no adiabatic process. Gao and Penlidis[6] (1996) indicated in relation to the Figure 3(c) that the experiment results is in a close range within experimental measurement error, considering the difficulty associated with particle number measurement determination, the model prediction should be considered satisfactory. The particle numbers were obtained by eqs. (43) and (44). These equations were solved together with the FVM in an iterative procedure to solve the whole set of equations. The particle number of the model prediction is approximately at 1.28×10^{18} particles/L (latex) as shown in Figure 3(c). The comparison of the three figures allows to conclude that the mathematical model is a good representation of the system and that the numerical FVM is a suitable one.

The results of simulation of the cumulative average molecular weight distribution versus conversion of monomer (Xj), without baffle (MnC0, MwC0; MnV0, MwV0) and with baffles (MnC6, MwC6; MnV6, MwV6) in isothermal (C) and no isothermal (V) conditions through of the TR are shown in Figure 6. The average molecular weights as shown in Figure 6(a–d) has different performance by reaction temperature and number of baffles effect. The number (Mn) and weight (Mw) molecular improve its distribution only marginally, when the baffles number increase inside the reactor. In fact, the strongest effect on the molecular number (Mn) as well as on molecular weight (Mw) molecular is due to the operation under no isothermal conditions. This claims to the development of reactor design able to carry out polymerization reaction with no isothermal conditions. The calculations of molecular weigh distribution were obtained through the value of initiator, radicals, conversion, particle numbers, etc., which were evaluated taking into account the temperature variations.

The comparative results of simulation of the polystyrene particles size of unswollen particle radius (*R*) versus length of the reactor (*Z*) without (V0) and with (V6) baffles in isothermal (C) and no isothermal (V) conditions are presented in Figure 7. The particle size in isothermal conditions show the highest size than in no isothermal conditions without (Nb = 0) and with (Nb = 6) baffles. The Figure 7(a,b) has similar behavior according to the temperature increment. When the baffle numbers increase in reactor, the particle size diminishes.

The simulation results of polymer viscosity distribution ($\ln(\mu)$ inside TR versus conversion of monomer

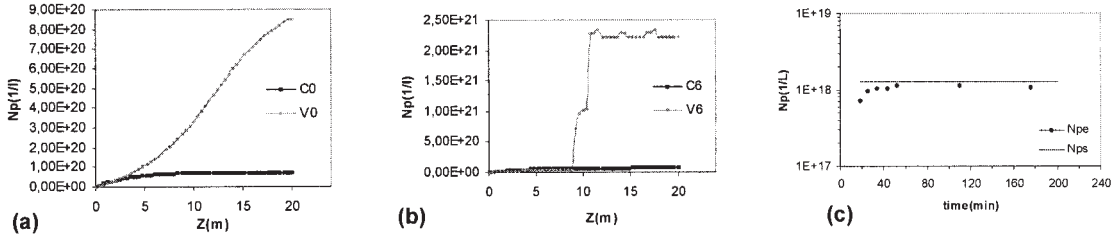

Figure 5 Number of particles (a) without baffles (Nb = 0) and (b) with baffles (Nb = 6) in isothermal (C) and no isothermal (V) conditions. (c) Number of particle validation at isothermic condition.

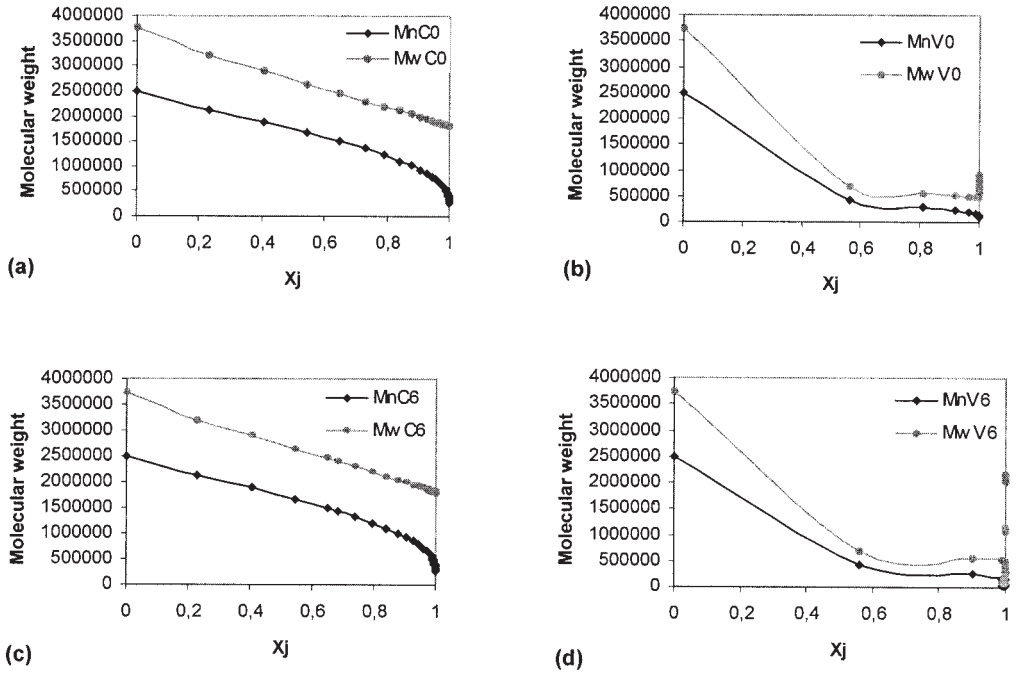

Figure 6 Molecular weight distribution; (a–b) without baffles (Nb = 0) and (c–d) with baffles (Nb = 6), both in isothermal (C) and no isothermal (V) conditions.

(Xj) and length of reactor (z) without (C0, V0) and with (C6, V6) baffles in isothermal (C) and no isothermal (V) conditions are shown in Figure 8. Figure 8(a, b) shows the same results, one expounds in function of conversion, other in function of length of reactor for better comparisons. The viscosity diminishes when the reaction temperature varies inside TR as shown in Figure 8(a–d). Also when the baffle numbers increase, the viscosity is lower than the viscosity without baffles. The mathematical model of the eq. (48) was used for estimate the viscosity [shown in Fig. 8(a,c)].[16]

Experimental data of conversion and particle number [Figs. 3(c) and 5(c)] were used to validate the proposed numerical solution procedure. Such data were for isothermal conditions and it was not found for the no isothermal conditions. Also, it is worth mentioning that neither laboratory scale nor plant date were found for the nonisothermal operation of styrene polymerization.

CONCLUSIONS

The performance of emulsion polymerization reactor in no isothermal condition showed better results than the reactor operated under isothermal conditions. Conversion and particle number values increase when the temperature increases. On the other hand, particle size and viscosity decrease when the temperature increases. The molecular weight distribution improves when the temperature vary inside the reactor. The results for no isothermal condition with baffles were better than for the system without baffles in relation to

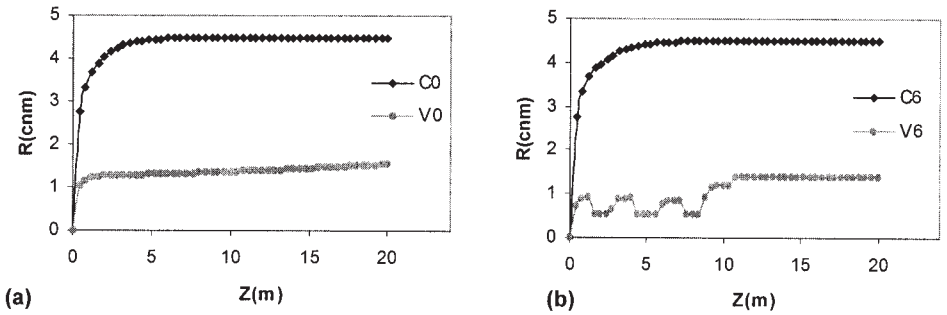

Figure 7 Average particle size distribution (a) without (Nb = 0) baffles and (b) with baffles (Nb = 6) in isothermal (C) and no isothermal (V) conditions.

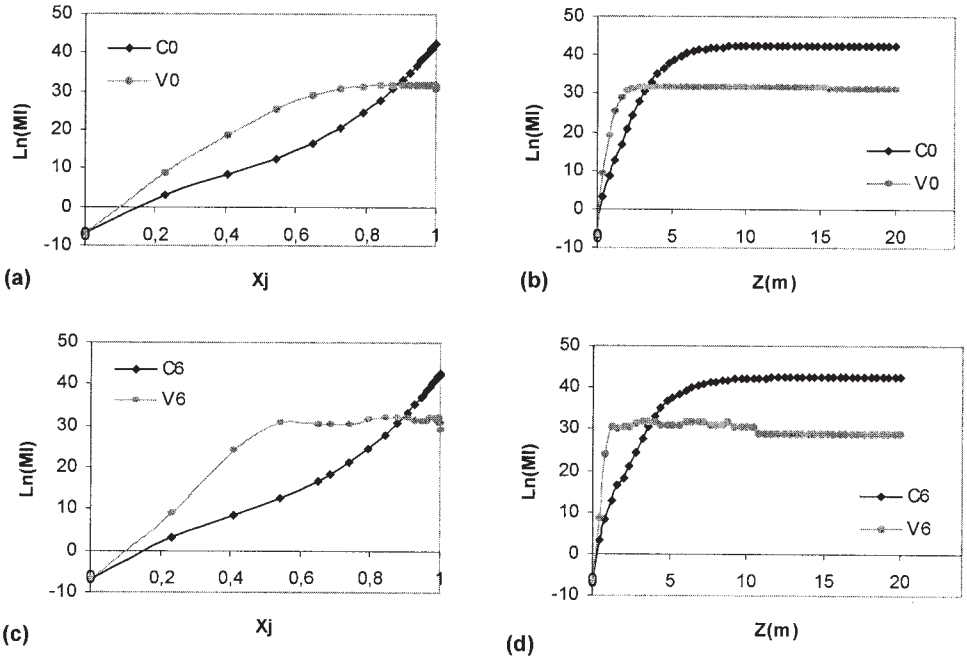

Figure 8 Viscosity distribution (a,b) without baffles (Nb = 0) and (c,d) with baffles (Nb = 6) in isothermal (C) and no isothermal (V) conditions.

desired properties, when looking of viscosity and average particle size. The differences are not large but they may have impact on the final product performance.

The reactor with baffles has, in fact, only a marginal effect on the molecular number distribution as well as on the molecular weight distribution. No experimental data were found by no isothermal conditions so that the validation of the solution process was carried out using the available data with isothermal reactor operation.

References

1. Paquet, D. A.; Ray, W. H. AIChE J 1994, 40, 73.
2. Chern, C. S. J Appl Polym Sci 1995, 56, 221.
3. Gilbert, R. G. Emulsion Polymerization, A Mechanistic Approach; Academic Press: London, 1995.
4. Scholtens, C. A. Process Development for Continuous Emulsion Copolymerization; CIP-DATA Library Technische Universities Eindhoven, Ter Verkrijging van de graad van Doctor, 2002.
5. Bockhorn, H. Mathematical Modeling, Ullmann's Encyclopedia of Industrial Chemistry; Wiley: New York, 1992; Vol. B1, Nr. 2.
6. Gao, J.; Penlidis, A. Prog Polym Sci 2002, 27, 403.
7. Maciel Filho, R.; Domingues, A. Presented at the 12th International Symposium on Chemical Reaction Engineering (ISCRE 12), Turin, Itália, 1992.
8. Siirola, J. J. AIChE J 1996, 23, 1.
9. Kiparissides, C. Chem Eng Sci 1996, 51, 1637.
10. Toledo, E. C. V. Modelagem, Simulação e Controle de Reatores Catalíticos de Leito Fixo, Tese de Doutorado, FEQ/UNICAMP, Campinas 1999.
11. Bataile, P.; Van, B. T.; Pham, Q. B. J Polym Sci Polym Chem Ed 1982, 20, 795.
12. Mendoza Marin, F. L. Modelagem, Simulação e Analise de Desempenho de Reatores Tubulares de Polimerização com Deflectores Angulares Internos; Tese de Doutorado, FEQ/UNICAMP, Campinas 2004.
13. Froment, G. F.; Bischoff, K. B. Chemical Reactor Analysis and Design, 2nd ed.; Wiley: New York, 1990.
14. Harkness, M. R. M.S. Thesis, Rensselaer Polytechnic Institute, Troy, New York, 1982.
15. Patankar, S. V. Numerical Heat Transfer and Fluid Flow; Hemisphere Publishing: New York, 1980.
16. Tucker, C. L., III. Fundamentals of Computer Modeling for Polymer Processing; Hanser: Munich, 1989.
17. Versteeg, H. K.; Malalasekera, W. An Introduction to Computational Fluid Dynamics, The Finite Volume Method, 2nd ed.; Longman: New York, 1998.